Colloids and Surfaces B: Biointerfaces 225 (2023) 113287

Contents lists available at ScienceDirect

Colloids and Surfaces B: Biointerfaces

journal homepage: www.elsevier.com/locate/colsurfb

Specific ion effects on copper electroplating

Walter Giurlani [a,b], Alberto Fidi [a], Erasmo Anselmi [a], Federico Pizzetti [a], Marco Bonechi [a,b], Emiliano Carretti [a,c], Pierandrea Lo Nostro [a,c,*], Massimo Innocenti [a,b,c,d,*]

[a] Dept. Chemistry "Ugo Schiff", University of Florence, via della Lastruccia 3, 50019 Sesto Fiorentino, Italy
[b] INSTM, Via G. Giusti 9, 50121 Firenze (FI), Italy
[c] CSGI, Via della Lastruccia 3, 50019 Sesto Fiorentino (FI), Italy
[d] ICCOM – CNR, via Madonna del Piano 10, 50019 Sesto Fiorentino, Italy

ARTICLE INFO

Keywords:
Electroplating
Specific ion effect
Copper
Nucleation
Growth

ABSTRACT

The main goal of this work is to open new perspectives in the field of electrodeposition and provide green alternatives to the electroplating industry. The effect of different anions (SO_4^{2-}, ClO_3, NO_3, ClO_4, BF_4^-, PF_6^-) in solution on the electrodeposition of copper was investigated. The solutions, containing only the copper precursor and the background electrolyte, were tailored to minimize the environmental impact and reduce the use of organic additives and surfactants. The study is based on electrochemical measurements carried out to verify that no metal complexation takes place. We assessed the nucleation and growth mechanism, we performed a morphological characterization through scanning electron microscopy and deposition efficiency by measuring the film thickness through X-ray fluorescence spectroscopy. Significant differences in the growth mechanism and in the morphology of the electrodeposited films, were observed as a function of the background electrolyte.

1. Introduction

Electroplating is a widely used industrial technique for both technical and decorative applications. The areas that most exploit this technique are electronics, automotive and fashion [1]. Although electrodeposition has been used for so long, the development of new processes and formulations is still a primary need in order to reduce the production costs and use of precious metals, and to obtain finishes with improved resistance to corrosion, wear and with the best aesthetic look [1]. Recently many national and international organizations devoted to the protection of the environment and of human health, set limits to the use of some metals and compounds to reduce the impact of these industrial processes [2]. Although electrodeposition is a simple electrochemical reaction, in order to obtain deposits with specific market-oriented features organic additives are necessary for different scopes, e.g., as brighteners, levelling and wetting agents. The formation of coatings with the same or improved features, obtained by reducing use of additives is not just a challenge, but a real "must" to guarantee a greater sustainability in electroplating processes and to comply with the current regulations [3,4].

In this work the effect of different supporting electrolytes (SEs) on copper electrodeposition was investigated. Copper was chosen because its deposition is well documented and, from the chemical standpoint, the formulation of the galvanic bath is simple. Then, in order to highlight the different effect due to the action of the electrolytes, the electroplating solution was formulated by using only copper sulphate and a single electrolyte without the addition of sulfuric acid or any further organic additive. These choices allowed us to highlight the different effect due to the action of the electrolytes. In detail, the main function of the SE is to increase the conductivity of the solution without having an electroactive behavior [5]. In principle, no effect on the deposition due to the change of an inert ion is expected. In particular, the main goal is to verify the occurrence of specific ion effects of SEs in the electrodeposition of copper, i.e., the non-trivial demonstration that the supporting electrolyte is not really "inert".

Specific ion effects were reported for the first time at the end of the nineteenth century by Hofmeister [6], and since then have been the subject of numerous studies on very different systems: from biochemical and colloidal systems [4] to polymers and soft matter materials [8–10], from bulk solutions to interfaces and living organisms [11,12]. Hofmeister proposed the ordering of cations and anions according to their effectiveness in precipitating egg yolk albumin [6]. More recently it was demonstrated that the Hofmeister series can reverse, or display partial changes in the trend, depending also on the hydrophobicity and charge

* Corresponding authors at: Dept. Chemistry "Ugo Schiff", University of Florence, via della Lastruccia 3, 50019 Sesto Fiorentino, Italy
E-mail addresses: pierandrea.lonostro@unifi.it (P. Lo Nostro), m.innocenti@unifi.it (M. Innocenti).

https://doi.org/10.1016/j.colsurfb.2023.113287
Received 31 December 2022; Received in revised form 16 March 2023; Accepted 28 March 2023
Available online 29 March 2023
0927-7765/© 2023 The Authors. Published by Elsevier B.V. This is an open access article under the CC BY license (http://creativecommons.org/licenses/by/4.0/).

of the involved interfaces [13].

In general ions can be ranked in a sequence according to their effect [14–16]. They can also be assigned a kosmotropic or chaotropic behavior [17]. Chaotropic ions are supposed to induce a destructuring effect on the hydrogen bonding of water (local structure), inversely kosmotropic species are thought to produce a remarkable structuring effect of water. To quantify these phenomena, the specific observable is related to some *descriptors*, i.e., physico-chemical parameters that characterize the effect of each ion [8]. They include the Gibbs free energy or the entropy of hydration, the polarizability, the molar surface tension increment, the partial molar volume, the Jones-Dole viscosity coefficient [11]. Usually, but not always, kosmotropes (such as F^- or Li^+) possess small polarizabilities and large Gibbs free energies of hydration. The opposite hold for chaotropes (such as I^- and Cs^+). A significant exception is the halate family (ClO_3^-, BrO_3^- and IO_3^-) [17].

Specific ion effects are determined by the interplay of hydration, electrostatics and dispersion forces. While dilute systems can be well described by electrostatic models, such as the Debye-Hückel model (for simple solutions) or the DLVO theory (for colloidal systems), at moderate or high salt concentration non-electrostatic forces come into play, e.g., dispersion forces that are highly specific. For further and more detailed discussions of Hofmeister phenomena the interested reader can refer to the cited literature and references therein [7,11,18–23].

Poorly solvated ions (chaotropes) likely adsorb more easily at the surface of an electrode [24] and can modify the conditions of deposition with a behavior similar to that of organic additives that are used in the plating baths to obtain compact and glossy deposits, like thiourea and sulfonic acid derivatives in copper plating or polyethyleneimine for silver plating [25–27].

Instead, there are only few works in the literature on specific ion effects for electrochemical depositions: i.e., Carneval studied the effect of different anions toward the copper deposition, but, since citrate and cyanide were used in that study, the main effect observed was due to their complexing behavior [28]. Vazquez-Arenas compared the effect of sulfate, perchlorate and nitrite, but no consideration was made with respect to the Hofmeister series or to specific ion effects [29]. More recently Vasiljevic reported on the influence of anion adsorption during the deposition of copper [30]: the use of low concentrations (0.25 mM) of halides strongly influenced the morphology of the copper film, but this behavior was probably due mainly to the partial formation of CuX precipitates on the electrode surface that modify the reaction pathway [31], and indeed specific ion effects typically occurs at concentrations $\geq$ 0.1 M [7].

In electrochemistry studies, most phenomena are discussed in terms of electrostatics. Instead, it has been shown that in Hofmeister (specific ion) studies electrostatic forces are screened whilst dispersion and hydration forces dominate. In fact, the formers are not ion specific and describe the physical chemistry of a solution only at very low salt concentration ($<$ 10 mM), in terms of charge and ion size. On the other hand, when the electrolyte concentration increases to moderate/high values and the system becomes overcrowded, then Coulomb forces vanish (the Debye screening length gets shorter and shorter) and ion specific short-range attractive interactions – including van der Waals, hydration, hydrogen bonding, π-ion interactions – emerge. We argue that this is the case also when the electrodeposition of a metal such as copper occurs in the presence of a relatively concentrated "inert" salt solution. In order to limit the number of experimental variables we chose to fix the cation (sodium) for all salts.

Regrettably several anions had to be excluded due to poor solubility, or to the formation of a precipitate or to a direct reaction with the Cu^{2+} ion. We extended the classical Hofmeister series [15] to more "exotic" ions [16,32]. The anions investigated in this study are SO_4^{2-}, ClO_3^-, NO_3^-, ClO_4^-, BF_4^- and PF_6^- and are reported in Fig. 1 sorted according to the Hofmeister series.

Other anions were initially considered: $H_2PO_4^-$, CO_3^{2-}, SCN^-, IO_3^-, F^-, I^-, but were discarded because they produce insoluble or not enough soluble compounds with Cu(II) at the concentrations commonly used for electroplating. Moreover, Cl^-, Br^- and BrO_3^- promote the formation of insoluble deposits (i.e., CuCl and CuBr) on the surface of the electrode rather than that of copper metal, while citrate has a strong complexing capacity.

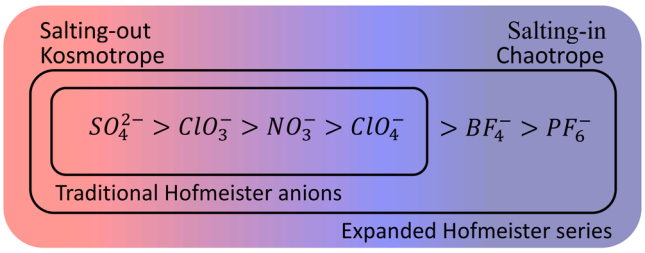

Fig. 1. Extended Hofmeister series of the anion used in this study based on the B_{JD} viscosity coefficient.

Different deposition experiments were carried out by using as SE different electrolytes, and the plating efficiency, morphology, and kinetics were monitored by SEM, XRF and electrochemical measurements. This study aims at opening new perspectives in the field of electrodeposition, both from a scientific and applicative point of view, and particularly with the perspective of providing ecological alternatives to the galvanic industry.

2. Experimental

The copper baths were prepared using 0.1 M $CuSO_4 \cdot 5\,H_2O$ (>99%, Alfa Aesar) and the appropriate quantity of sodium salts in order to achieve 1 M for each anion, in particular Na_2SO_4 (> 99%, Merck), $NaClO_3$ (>99%, Sigma-Aldrich), $NaNO_3$ (>99%, Merck), $NaClO_4$ (>99% Fluka), $NaBF_4$ (>99% Fluka) and $NaPF_6$ (>99%, Alfa Aesar) were used. All solutions were prepared with Milli-Q water from "Sartorius Arium Mini" (0.055 μS/cm).

2.1. Electrochemical analysis

The conductivity of the baths was measured with a Metrohm 712 Conductometer (cell constant = 0.79 cm^{-1}), each sample was measured five times. A conventional three-electrode cell was used for the electrochemical experiments. A glassy carbon (GC) electrode tip (Metrohm) was used as working electrode (WE), with a 3.14 mm^2 exposed area, unless otherwise indicated. Platinum wire was used as a counter electrode (CE), and an Ag/AgCl saturated KCl (−0.045 V vs SHE) as the reference electrode (RE). Before each experiment the working electrode was regenerated by mechanical polishing using alumina powder (0.3 μm), rinsed with ultrapure water, and then cleaned with a cyclovoltammetry procedure in a 0.5 M H_2SO_4 solution repeatedly scanning the potential between + 1 V and − 1 V at a rate of 50 mV/s. After the cleaning procedure the activation degree of the electrode was evaluated by looking at the difference in the peak potential for the redox couple of ferro/ferricyanide, which is expected to be close to 60 mV, by performing a cyclic voltammetry scan in a $K_4Fe(CN)_6$ 1 mM + $K_3Fe(CN)_6$ 1 mM aqueous solution in KCl 1 M. All solution was thermostated to 25 °C and degassed by bubbling nitrogen gas. A nitrogen atmosphere was maintained above the solution during the measurements. The electrochemical experiments, cyclic voltammetry and chronoamperometry, were performed using a μAutolab PGSTAT204 potentiostat/galvanostat, coupled to NOVA 2.1.4 software. Same set-up was used to perform the depositions for the further ex situ characterizations, only the GC working electrode has been changed: a wider electrode with a radius of 5 mm was used.

2.2. Copper deposition

The samples were prepared performing a potentiostatic deposition from the baths containing 0.1 M $CuSO_4$ and 1 M of Na_2SO_4, $NaClO_3$, $NaNO_3$, $NaClO_4$, $NaBF_4$ and $NaPF_6$ at the peak potential recorded in the corresponding CV Fig. 2. To obtain deposits with comparable thickness the Faraday's law of electrolysis was used. The charge required to obtain the desired deposit thickness was obtained using Eq. 1.

$$Q = \frac{dS\rho zF}{M} \quad (1)$$

Where d is the thickness of the deposit, S is the exposed area of the electrode, ρ the density of the metal, z is the number of exchanged electrons, F is the Faradays constant and M is the molar mass of the metal.

The substrate used for the deposition was a glassy carbon disk with a diameter of 10 mm. To obtain a deposit with an equivalent thickness of 200 nm we calculated a charge of − 0.4274 C. This value of charge was set as the cut-off for the depositions.

2.3. Deposit characterization techniques

The thickness of the copper deposits was determined through X-ray fluorescence (XRF) measurements [33] by using a Bowman B Series XRF spectrometer using an acquisition time of 60 s, 50 kV tube voltage, 0.8 mA tube current, and a collimator of 0.6 mm in diameter. The average equivalent thickness of all copper deposits, performed in five distinct points on each sample, was confirmed to be 200 ± 0.02 nm.

The morphology and distribution of electrodeposited copper coating were examined using a Hitachi SU3800 scanning electronic microscope (SEM) equipped with an EDS spectrometer (Ultim Max 40). SEM images have been processed with ImageJ software [34].

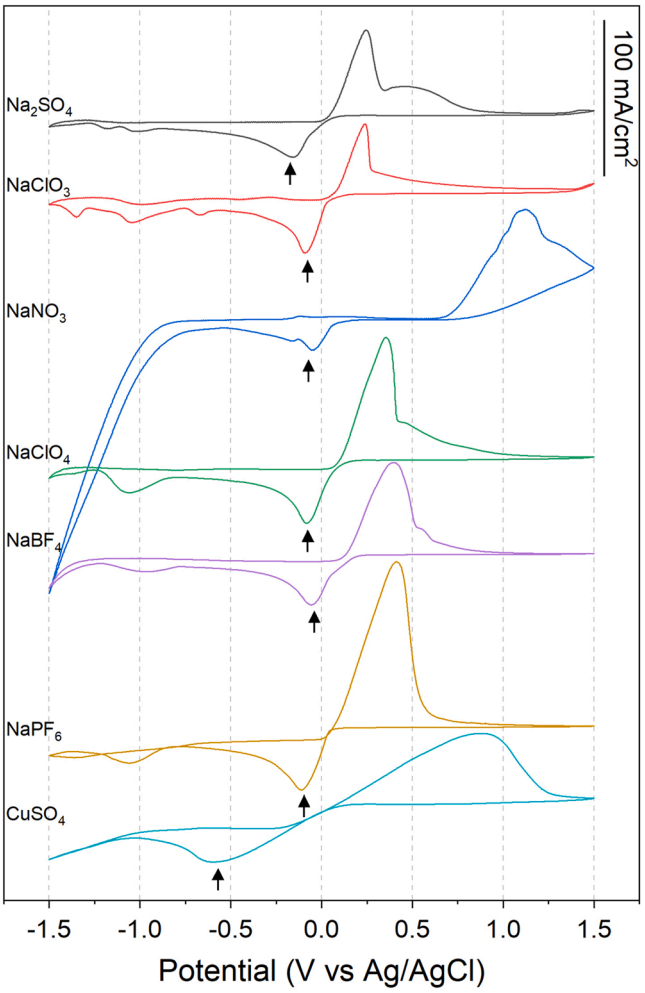

Fig. 2. CVs of the solutions containing the Cu^{2+} salt and the investigated SEs. For comparison the solution containing only $CuSO_4$ 0.1 M is shown at the bottom. The black arrows indicate the reduction peaks of copper.

3. Results

Table 1 lists the conductivity and the pH of the solutions. The conductivity of the solution containing $CuSO_4$ only has a conductivity of about one order of magnitude lower than the solution containing the SEs due to its lower ionic strength. The solutions containing the SEs have a relatively similar conductivity, between 65 and 73 μS/cm, except for the solution of Na_2SO_4 with a value higher than 81 μS/cm because its van't Hoff coefficient i is 3 instead of 2. The pH of the solutions was in the 4.3 ± 0.5 range, sufficiently narrow for copper deposition. Only $NaPF_6$ produced a more acidic solution with a pH of 2.2. Anyway, the pH was not adjusted to keep fixed the ionic strength of the solutions (Table 1).

3.1. Cyclic voltammetry measurements

The CV measurement on the GC electrode were performed between − 1.5 and 1.5 V, starting from 0.3 V moving to negative potentials with a scan rate of 100 mV/s. The solutions containing only the SE, without the copper precursor, were first tested for possible faradic processes that could have an effect on the reduction of the metal or the degradation of the SE. The measurements were compared to the $CuSO_4$ solution (Fig. S1): no appreciable peak was detected in solutions containing the SEs alone. Only in the case of nitrate a small discharge took place at very negative potential, due to the reduction of the nitrate ion [27], which can be considered negligible respect to the copper reduction that starts at about 0 V.

Then, the solutions containing both the copper and the SE (Fig. 2) were analyzed. For each solution a strong cathodic and anodic peak is visible, due to the Cu^{2+}/Cu couple.

The shape and the position of the anodic peak varied with the anion and the split suggests that the reaction occurs in a one-electron process ($Cu \rightarrow Cu^{+} \rightarrow Cu^{2+}$) rather than by a direct two-electron process ($Cu \rightarrow Cu^{2+}$). Regarding the deposition process the onset of the reduction is almost identical for all solutions (Table 1), indicating that the complexation of Cu^{2+} ions by the SEs anions is negligible. However for the SE-free system, the reduction peak is much less sharp and falls at considerably lower potentials due to the lower conductivity of the solution [35]. The potential value of the peak for to the copper reduction

Table 1
Conductivity (σ), pH (± 0.05), onsets and peaks potentials recorded in the CVs measurements of the solutions at 25 °C. The concentration of all SEs is 1 M.

Electrolyte	σ (μS/cm)	Ionic strength (M)	pH	Onset potential (V)	Peak potential (V)
$CuSO_4$	8.01 ± 0.04	0.4	4.16	0.10	-0.56
$CuSO_4$ + Na_2SO_4	81.70 ± 0.57	0.7	4.76	0.06	-0.15
$CuSO_4$ + $NaClO_3$	65.89 ± 0.25	0.5	4.00	0.04	-0.11
$CuSO_4$ + $NaNO_3$	71.69 ± 0.24	0.5	4.00	0.02	-0.11
$CuSO_4$ + $NaClO_4$	72.21 ± 0.21	0.5	4.47	0.07	-0.09
$CuSO_4$ + $NaBF_4$	69.60 ± 0.27	0.5	3.93	0.09	-0.05
$CuSO_4$ + $NaPF_6$	73.07 ± 0.23	0.5	2.22	0.07	-0.11

in the presence of the SEs, falls in a relatively narrow range, − 0.15 < V < − 0.05 (see Table 1). The sequence of the potentials parallels the Hofmeister series: as the kosmotropic character of the anions of the SEs increases, the peak shifts toward a lower potential. Only the solution containing $NaPF_6$ does not follow this trend. However, the behavior of PF_6^- is not deeply understood due to its nature, that can justify the deviation from the Hofmeister series [16].

At more negative potentials respect to the reduction peak of copper (indicated by black arrows in Fig. 2), other less intense peaks are observed. These peaks were not previously observed in the absence of the salt (light blue curve in Fig. S1). A peak around − 1.0 V was observed in each solution. This peak is not always present in the first scan and is presumably due to the partial formation of copper oxide during the anodic scanning, that is then reduced at higher potentials than the Cu^{2+} ion.

In the case of the two investigated chlorinated SEs (ClO_3^- and ClO_4^-), that thermodynamically are oxidizing species but kinetically inert, other two peaks were observed around − 0.65 V and − 1.35 V. These peaks are assigned to the partial reduction to chloride catalyzed by the metal [36,37]. Copper nuclei have a similar catalytic behavior also towards nitrate [27,29] with an intense cathodic discharge below − 0.8 V.

The anodic part of the CV is not the focus of this study but was kept for completeness. Widening the scan range to more negative potentials had an influence also on the oxidative behavior of the metal, probably due to the formation of new species. The most noticeable example can be observed in the case of nitrate, with an anodic peak of copper above 1.0 V.

3.2. Chronoamperometric measurements

We investigated the mechanism of nucleation and growth of copper by performing chronoamperometric measurements for 30 s at the potential corresponding to the peak potential recorded in the CVs (see Table 1). For all solutions we obtained the typical trend expected for the electrodeposition of a metal [38]. In the case of $NaClO_3$ two peaks are present, one of which is probably due to the partial formation of CuCl and whose presence will be confirmed by the elemental analysis of the deposit. Fig. 3a shows the current transient recorded during the

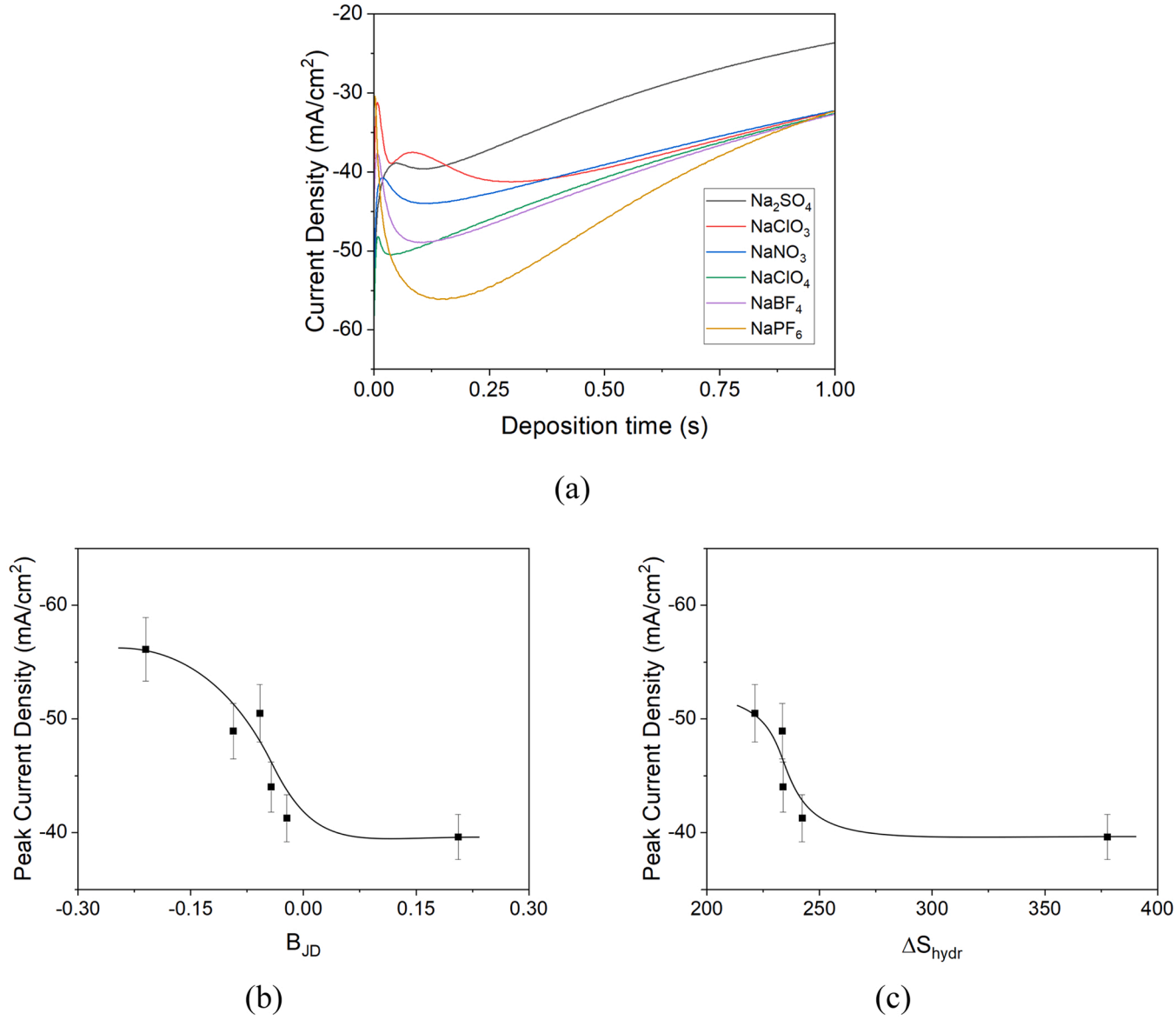

Fig. 3. Chronoamperometric measurements performed on the solutions containing Cu^{2+} and SEs: a) Current transient recorded during the deposition; b) Peak current density (PCD) as a function of the Jones-Dole viscosity coefficient; c) Peak current density (PCD) as a function of the entropy change of hydration. The curves are guidelines for the eye.

deposition, whilst Fig. 3b and c show the variation of the peak current density as a function of two descriptors, the Jones-Dole viscosity coefficient (B_{JD}, in L·mol^{-1}) [39] and the entropy change of hydration ($\Delta_{hydr}S^{\circ}$, in J·mol^{-1}·K^{-1}) [40]. The values of peak current density, B_{JD} and $\Delta_{hydr}S^{\circ}$ are listed in Table S1. The Jones-Dole viscosity coefficient is defined according to Eq. 2 [8,17,39]:

$$\eta = \eta_w\left(1 + a\sqrt{c} + B_{JD}c\right) \tag{2}$$

Where η, η_w and a are the viscosity of the salt solution at concentration c, that of pure water at the same temperature, and a constant that does not depend on the solute, respectively.

The data were fitted using a nucleation and growth model. The electrodeposition process can be described with two extreme scenarios: i) instantaneous nucleation and ii) progressive nucleation. In the former the nuclei are produced in the first instants of the deposition and then grow without increasing their number, in the latter new seeds are continuously formed during the deposition. The most common model for the interpretation of the current transient and to identify whether a nucleation is instantaneous or progressive, was developed by Scharifker and Hill [41]. This model assumes the formation of 3D hemispherical nuclei and their coalescence with a diffusion-controlled deposition.

Generally, the theoretical instantaneous (Eq. 3) and progressive (Eq. 4) curves obtained from the model are visually compared to the normalized experimental curves to identify the type of nucleation. The normalization is performed by dividing the measured current density values J by the maximum value, J_m, and the time values t by the time at which J_m occurs, t_m.

$$\frac{J^2}{J_m^2} = 1.9542\left(\frac{t}{t_m}\right)^{-1}\left(1 - \exp\left(-1.2564\left(\frac{t}{t_m}\right)\right)\right) \tag{3}$$

$$\frac{J^2}{J_m^2} = 1.2254\left(\frac{t}{t_m}\right)^{-1}\left(1 - \exp\left(-2.3367\left(\frac{t}{t_m}\right)^2\right)\right) \tag{4}$$

If a mixed nucleation occurs the data falls between the two curves and can be fitted using the Scharifker-Mostany (SM) equation [42], which describes the progress of the current J_{3Ddc} in a three dimensional deposition diffusion-controlled process (Eq. 5).

$$J_{3Ddc}(t) = zFc\sqrt{\frac{D}{\pi t}}\left(1 - \exp\left(-N_0\pi D\sqrt{\frac{8\pi cM}{\rho}}\left(t - \frac{1-\exp(-At)}{A}\right)\right)\right) \tag{5}$$

Where D is the diffusion coefficient, N_0 is the number density of active sites and A is the nucleation rate per active site, respectively.

Side reactions and mixed charge–mass transport can cause deviations from the SM model [43,44]. For this reason, two other contributions should be considered for the total current. The first is J_{PR} (Eq. 6), that takes into account parasitic processes including the reduction of hydrogen ion and dissolved oxygen [45].

$$J_{PR}(t) = P_1\left(1 - \exp\left(-N_0\pi D\sqrt{\frac{8\pi cM}{\rho}}\left(t - \frac{1-\exp(-At)}{A}\right)\right)\right) \tag{6}$$

P_1 is a fitting parameter that includes the charge transfer and the rate constant of the parasitic reaction.

The second contribution to the total current is provided by the adsorption/desorption of ion species and ion transfer current [46], J_{IT} (Eq. 7), which compensates for the fact that the process is not under a full diffusion-control. Vazquez named this contribution as electron transfer and, for the deposition of copper, attributes it to the slow intermediate step of the double electron reduction of copper that involves the production of Cu(I) [29].

$$J_{IT}(t) = k_1\exp(-k_2t) \tag{7}$$

Therefore, the total current density of copper electrodeposition is:

$$J_{tot} = J_{3Ddc} + J_{PR} + J_{IT} \tag{8}$$

After the fitting process the J_{3Ddc} contribution has been extrapolated and normalized (Fig. 4a). The nucleation and growth mechanism are different in the presence of different SEs and follow the Hofmeister series (Fig. 4a inset).

The SM model introduce the dimensionless α parameter (Eq. 9) that reflects the progressive or instantaneous character of a deposition. The values of α can range from 0 to ∞ , for a pure instantaneous and for a pure progressive mechanism, respectively.

$$\alpha = \frac{N_0\pi D}{A}\sqrt{\frac{8\pi cM}{\rho}} \tag{9}$$

We calculated the α values (see Fig. 4b and Table S2) and confirmed the sequence of the Hofmeister series. α changes significantly along the series of the anions, with a basically instantaneous nucleation for hexafluorophosphate and progressive nucleation for sulphate, nitrate, and chlorate. Perchlorate and tetrafluoroborate seem to induce an intermediate mechanism.

3.3. SEM analysis

SEM analyses were performed on the copper deposits obtained setting a cut-off charge of − 0.4274 C, equivalent to a thickness of 200 nm. SEM images showed the presence of large and isolated crystals with dimensions in the ranging between 1 and 10 μm (Fig. 5).

The absence of a 200 nm continuous film, expected from the charge used for the electrodeposition of the copper, is probably due to the nature of the GC substrate. We recall that the deposition charge and the XRF measurement refer to the equivalent average thickness of the deposit. The crystals showed different shapes and morphologies depending on the SE. We found two different types of crystals in each sample: cuboctahedrons and dendritic, whose relative amount changes with the solution composition. While the cuboctahedrons are very similar in shape in all the investigated samples, the dendritic particles significantly change with the electrolyte. The deposits obtained from Na_2SO_4, $NaClO_3$ and $NaNO_3$ (Fig. 5a, b and c, respectively), look more globular and tend to coalesce, while the deposits obtained from $NaClO_4$ (Fig. 5d), $NaBF_4$ (Fig. 5e) and $NaPF_6$ (Fig. 5f), are sharper, needle-like and less aggregated.

4. Discussion

In this section we review and discuss the different mechanisms through which the different salts can produce the observed results.

The results suggest that the effects of different anions on the electroplating of copper are not ruled by Coulomb's electrostatics but rather by their specific behavior, mainly their hydration and adsorption at the electrode surface (Fig. 3b,c).

In complex systems, different and often contrasted processes may occur simultaneously [47] and their overall effect can result in partial reordering and total inversions in the series [7,48]. The reason of such anomalies and discrepancies may reside on two or more concurrent and conflicting mechanisms, for example adsorption of ions at interfaces, onset of non-electrostatic interactions, hydration, ion binding and bridging, formation of ion pairs and more [8,17,20]. They all participate to the global effect, but each mechanism is ion specific and can produce a different position of a particular ion in the Hofmeister sequence. As a matter of fact it is not rare to find systems and phenomena where the trend that represents the effectiveness of the ions has the shape of a bell (usually referred to as the "volcano plot" [49]), meaning that kosmotropes and chaotropes have similar effects and intermediate ions (mild kosmotropic and moderate chaotropic) produce a much stronger effect [50].

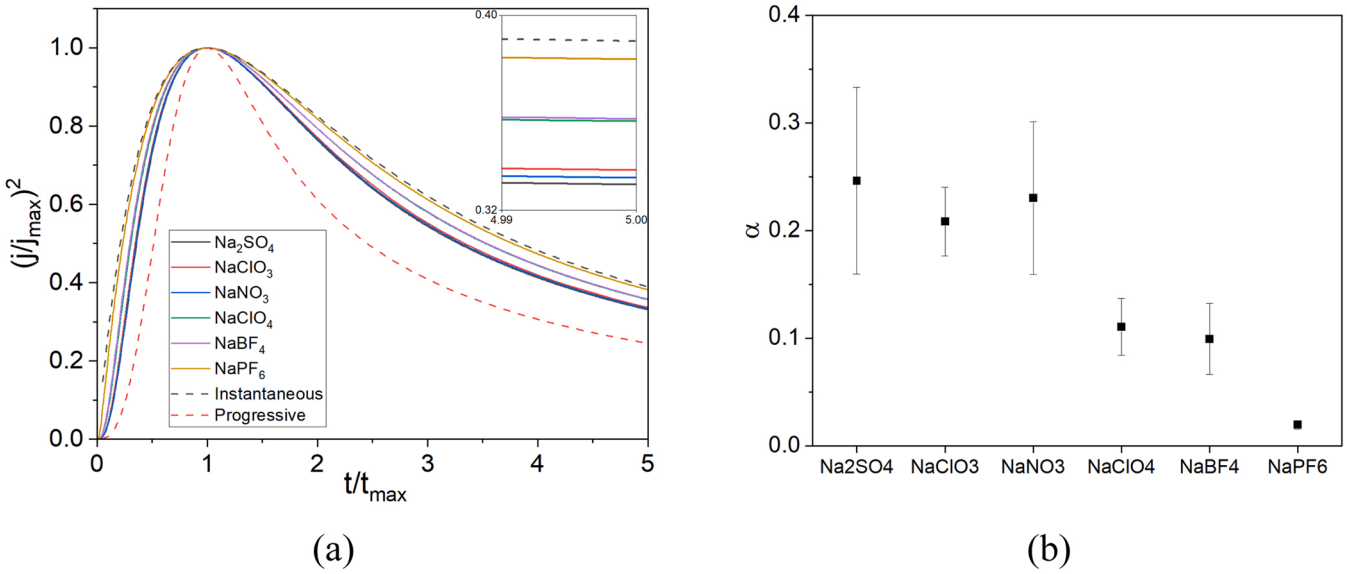

Fig. 4. a) Current transient extrapolated from the measurement according to Eq. 5 and Eq. 6 and normalized respect to the peak current and time. Pure instantaneous and progressive growth Scharifker-Hills curves are reported for comparison. A magnification is reported in the inset to better identify the sequence; b) α parameter as function of the electrolyte.

The more chaotropic an ion, the lower its hydration [17] and viscosity, hence the deposition of the metal is favored. On the other hand, the more chaotropic ions have also a high adsorption capacity at interfaces [47]. In particular, by adsorbing at the electrode surface, they tend to slow down and modify the growth of the metal. The combined action of these two opposite phenomena generates an overall result (see Table 1) in which the deposition potential values fall within a narrow range because the two processes weaken one each other. The combination of these two contrasting mechanisms can also be traced in the SEM images (Fig. 5a-f) in which different shapes of copper crystals are observed within the same deposit.

As outlined by Franklin in his review [51] a generic additive can be regarded as "dirt" that interferes in the electroplating process because of its interfacial features and "not its chemistry".

An interesting explanation involves the hydration of the Cu(II) ion. In fact the reduction of the aquo complex $[Cu(H_2O)_6]^{2+}$ needs either a partial dehydration or a substitution of some water molecules with ion bridges. In this view the activity of sulfate in favoring the partial desolvation of the copper ion is certainly stronger than in the case of chaotropic species like nitrate or tetrafluoroborate. Moreover, the adsorption of an anion can be competitive with that of the Cu(II) ions at the electrode interface. This is particularly true in the case of chaotropic anions, that possess lower hydration energies and lower molar surface tension increments defined as $\sigma = \frac{\partial \gamma}{\partial c}$ [6]. In passing we also recall that the great change in the dielectric constant between the bulk solution and the electrode interface produces an image potential that attracts some ions more efficiently than others [7]. Complexation and ion pairing do not seem to be relevant in the present study.

Another contribution may derive from the presence of dissolved gases that form micro- and nanobubbles in solution [23]. Apparently, their effect involves the formation of a hydrophobic layer around the electrode that promotes the dehydration of the cation before the reduction. It has been demonstrated that different combination of cations and anions can stabilize the bubbles and inhibit their fusion. In particular, Na_2SO_4 and $NaNO_3$ inhibit the coalescence and stabilize bubbles, while $NaClO_3$ and $NaClO_4$ are not effective (see Table 2 in [52]). The formation of tiny H_2 bubbles right at the surface of the cathode can further increase this effect. We recall here the well-known effect of additives on hydrogen evolution and brightness of Ni, Pt and Cd layers: the brightest deposits were made in regions where the evolution of H_2 was minimal [53]. Moreover, it is known that the properties of electrolytic solutions modify the quantity of evolved hydrogen during deposition, influencing the morphology of copper electrodeposits [54].

Specific adsorption of anions at the water/metal interface (Hg, Pt and Au) was also discussed by Conway [47]. Chemisorption of ions at metal surfaces is thought to be related to a charge transfer mechanism that occurs between the metal and the valence-electron orbitals. Conway, in his paper, wrote: "Hence, the larger is the ion the more easily are its lone-pair orbitals available for direct contact with the metal surface assisted by deformation of the solvation co-sphere" [47]. We show here that it is not really matter of the ion size, but rather of the hydration and interfacial properties of the anions.

5. Conclusions

In this study, we investigated the effect of different supporting electrolytes on copper plating by considering different aspects of copper electrodeposition. Six different Na^+ salts were used, with different anions that do not form coordination complexes with Cu(II). The Cu^{2+} concentration is compatible with that of the electroplating industry.

Interesting differences were found in the nucleation and growth process by analyzing the current transients during deposition. Apparently the more kosmotropic salts promote a progressive nucleation (generally preferred in electroplating [25,27]) while the more chaotropic salts favor an instant nucleation. The results suggest that ionic hydration and interfacial properties have the most important impact on the investigated process. Important differences in the shape of the deposited crystals were also found through SEM measurements.

These results pave the way to the formulation of new electroplating baths with a lower use of organic additives, and therefore for a more sustainable and green process.

CRediT authorship contribution statement

Conceptualization, W.G, P.L.N. and M.I.; methodology, W.G. and P.L.N.; validation, W.G., E.C. and P.L.N.; formal analysis, W.G. and F.P.; investigation, A.F. and E.A.; resources, W.G. and P.L.N.; data curation, W.G., E.C. and P.L.N.; writing—original draft preparation, W.G., A.F., E.A., P.L.N.; writing—review and editing, W.G., M.B., E.C. P.L.N and M.I.;

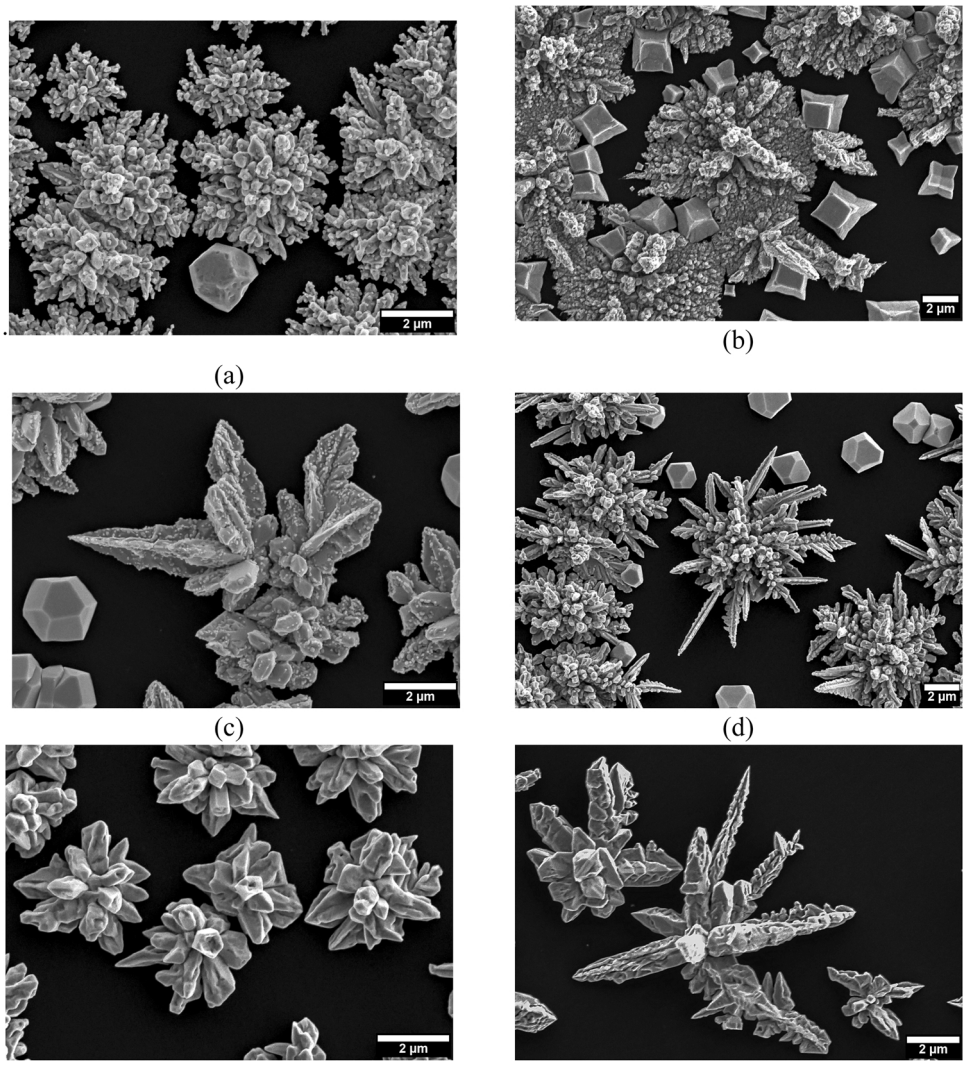

Fig. 5. SEM analysis of the deposits obtained with a deposition charge of − 0.4274 C with the various electrolytes: a) Na_2SO_4; b) $NaClO_3$; c) $NaNO_3$; d) $NaClO_4$; e) $NaBF_4$; f) $NaPF_6$.

supervision, W.G., P.L.N and M.I; project administration, M.I.; funding acquisition, M.I. All authors have read and agreed to the published version of the manuscript.

Declaration of Competing Interest

The authors declare that they have no known competing financial interests or personal relationships that could have appeared to influence the work reported in this paper.

Data Availability

Data will be made available on request.

Acknowledgments

This research was funded by Regione Toscana POR CreO FESR 2014-2020, Azione 1.1.5 sub A1) Bando 2 "Progetti di Ricerca e Sviluppo delle MPMI " which made possible the project "Galvanica Intelligente per Gioielli e Accessori 4.0″ (GIGA 4.0) CUP 3553.04032020.158000105_1242, CIPE D64E20003740009.

Appendix A. Supporting information

Supplementary data associated with this article can be found in the online version at doi:10.1016/j.colsurfb.2023.113287.

References

[1] W. Giurlani, G. Zangari, F. Gambinossi, M. Passaponti, E. Salvietti, F. Di Benedetto, S. Caporali, M. Innocenti, Electroplating for decorative applications: recent trends in research and development, Coatings 8 (2018) 260.
[2] European Commission, REACH - List of Amendments to Annex XVII - Restrictions, 2022.
[3] E. Mariani, W. Giurlani, M. Bonechi, V. Dell'Aquila, M. Innocenti, A systematic study of pulse and pulse reverse plating on acid copper bath for decorative and functional applications, Sci. Rep. 12 (2022) 18175.
[4] E. De Beni, W. Giurlani, L. Fabbri, R. Emanuele, S. Santini, C. Sarti, T. Martellini, E. Piciollo, A. Cincinelli, M. Innocenti, Graphene-based nanomaterials in the electroplating industry: a suitable choice for heavy metal removal from wastewater, Chemosphere 292 (2022), 133448.
[5] The IUPAC Compendium of Chemical Terminology, 1491 (2014) 6149, International Union of Pure and Applied Chemistry, Research Triangle Park, NC.
[6] W. Kunz, P. Lo Nostro, B.W. Ninham, The present state of affairs with Hofmeister effects, Curr. Opin. Colloid Interface Sci. 9 (2004) 1–18.
[7] P. Lo Nostro, B.W. Ninham, Hofmeister phenomena: an update on ion specificity in biology, Chem. Rev. 112 (2012) 2286–2322.
[8] D. Tatini, D. Ciardi, C. Sofroniou, B.W. Ninham, P. Lo Nostro, Physicochemical characterization of green sodium oleate-based formulations. Part 2. Effect of anions, J. Colloid Interface Sci. 617 (2022) 399–408.

[9] P. Lo Nostro, N. Peruzzi, M. Severi, B.W. Ninham, P. Baglioni, Asymmetric partitioning of anions in lysozyme dispersions, J. Am. Chem. Soc. 132 (2010) 6571–6577.
[10] M. Bonechi, M. Innocenti, D. Vanossi, C. Fontanesi, The fundamental and underrated role of the base electrolyte in the polymerization mechanism. The resorcinol case study, J. Phys. Chem. A 125 (2021) 34–42.
[11] M.A. Budroni, F. Rossi, N. Marchettini, F. Wodlei, P. Lo Nostro, M. Rustici, Hofmeister effect in self-organized chemical systems, J. Phys. Chem. B 124 (2020) 9658–9667.
[12] P. Lo Nostro, B.W. Ninham, E. Carretti, L. Dei, P. Baglioni, Specific anion effects in Artemia salina, Chemosphere 135 (2015) 335–340.
[13] N. Schwierz, D. Horinek, U. Sivan, R.R. Netz, Reversed Hofmeister series—the rule rather than the exception, Curr. Opin. Colloid Interface Sci. 23 (2016) 10–18.
[14] V. Mazzini, V.S.J. Craig, What is the fundamental ion-specific series for anions and cations? Ion specificity in standard partial molar volumes of electrolytes and electrostriction in water and non-aqueous solvents, Chem. Sci. 10 (2019) 3430–3433.
[15] B. Kang, H. Tang, Z. Zhao, S. Song, Hofmeister series: insights of ion specificity from amphiphilic assembly and interface property, ACS Omega 5 (2020) 6229–6239 (2020).
[16] J.H. Jordan, C.L.D. Gibb, A. Wishard, T. Pham, B.C. Gibb, Ion–Hydrocarbon and/or Ion–Ion Interactions: direct and reverse Hofmeister effects in a synthetic host, J. Am. Chem. Soc. 140 (2018) 4092–4099.
[17] M. Acar, D. Tatini, B.W. Ninham, F. Rossi, N. Marchettini, P. Lo Nostro, The lyotropic natures of halates: an experimental study, Molecules 27 (2022) 8519.
[18] A. Salis, M. Cristina Pinna, D. Bilaničová, M. Monduzzi, P. Lo Nostro, B.W. Ninham, Specific anion effects on glass electrode pH measurements of buffer solutions: bulk and surface phenomena, J. Phys. Chem. B 110 (2006) 2949–2956.
[19] A. Salis, L. Cappai, C. Carucci, D.F. Parsons, M. Monduzzi, Specific buffer effects on the intermolecular interactions among protein molecules at physiological pH, J. Phys. Chem. Lett. 11 (2020) 6805–6811.
[20] B.W. Ninham, V. Yaminsky, Ion binding and ion specificity: the hofmeister effect and onsager and lifshitz theories, Langmuir 13 (1997) 2097–2108.
[21] B.W. Ninham, R.M. Pashley, P. Lo Nostro, Surfaces forces: Changing concepts and complexity with dissolved gas, bubbles, salt and heat, Curr. Opin. Colloid Interface Sci. 27 (2017) 25–32 (2017).
[22] B.W. Ninham, The biological sciences divide, and the age of unreason, Substantia 1 (2017) 7–24.
[23] B.W. Ninham, P. Lo Nostro, Unexpected properties of degassed solutions, J. Phys. Chem. B 124 (2020) 7872–7878 (2020).
[24] N. Mittal, T. Benselfelt, F. Ansari, K. Gordeyeva, S.V. Roth, L. Wågberg, L. D. Söderberg, Ion-specific assembly of strong, tough, and stiff biofibers, Angew. Chem. Int. Ed. 58 (2019) 18562–18569.
[25] L. Fabbri, W. Giurlani, G. Mencherini, A. De Luca, M. Passaponti, E. Piciollo, C. Fontanesi, A. Caneschi, M. Innocenti, Optimisation of thiourea concentration in a decorative copper plating acid bath based on methanesulfonic electrolyte, Coatings 12 (2022) 376.
[26] C. Gabrielli, P. Moçotéguy, H. Perrot, D. Nieto-Sanz, A. Zdunek, An investigation of copper interconnect deposition bath ageing by electrochemical impedance spectroscopy, J. Appl. Electrochem 38 (2008) 457–468.
[27] F. Pizzetti, E. Salvietti, W. Giurlani, R. Emanuele, C. Fontanesi, M. Innocenti, Cyanide-free silver electrodeposition with polyethyleneimine and 5,5-dimethyl-hydantoin as organic additives for an environmentally friendly formulation, J. Electroanal. Chem. 911 (2022), 116196.
[28] G. Carneval, J.B. de Cusminsky, The influence of the anion on copper electrocrystallization, J. Electrochem. Soc. 128 (1981) 1215–1221.
[29] J. Vazquez-Arenas, G. Vázquez, A.M. Meléndez, I. González, The Effect of the Cu^{2+}/Cu^{+} Step on Copper Electrocrystallization in Acid Noncomplexing Electrolytes, J. Electrochem. Soc. 154 (2007) D473.
[30] N. Vasiljevic, M. Wood, P.J. Heard, W. Schwarzacher, The influence of specific anion adsorption on the surface roughness of electrodeposited polycrystalline Cu films, J. Electrochem. Soc. 157 (2010) D193.
[31] W. Shao, G. Pattanaik, G. Zangari, Influence of chloride anions on the mechanism of copper electrodeposition from acidic sulfate electrolytes, J. Electrochem. Soc. 154 (2007) D201.
[32] K.I. Assaf, W.M. Nau, The chaotropic effect as an assembly motif in chemistry, Angew. Chem. Int. Ed. 57 (2018) 13968–13981.
[33] W. Giurlani, E. Berretti, A. Lavacchi, M. Innocenti, Thickness determination of metal multilayers by ED-XRF multivariate analysis using Monte Carlo simulated standards, Anal. Chim. Acta 1130 (2020) 72–79.
[34] Image J. Available online: ⟨https://imagej.nih.gov/ij/⟩ (accessed on Dec 10, 2022).
[35] N.G. Tsierkezos, U. Ritter, Influence of concentration of supporting electrolyte on electrochemistry of redox systems on multi-walled carbon nanotubes, Phys. Chem. Liq. 50 (2012) 661–668.
[36] M. Ujvári, G.G. Láng, in Encyclopedia of Interfacial Chemistry, Elsevier, Amsterdam, 2018, pp. 95–106.
[37] J. Lei, S. Rudenja, N. Magtoto, J.A. Kelber, Cu electrodeposition on Ru)0001): perchlorate dissociation and its effects on Cu deposition, Thin Solid Films 497 (2006) 121–129.
[38] L. Heerman, A. Tarallo, Theory of the chronoamperometric transient for electrochemical nucleation with diffusion-controlled growth, J. Electroanal. Chem. 470 (1999) 70–76.
[39] H.D.B. Jenkins, Y. Marcus, Viscosity B-coefficients of ions in solution, Chem. Rev. 95 (1995) 2695–2724.
[40] Y. Marcus, Thermodynamics of solvation of ions. Part 5.-Gibbs free energy of hydration at 298.15 K, J. Chem. Soc., Faraday Trans. 87 (1991) 2995–2999.
[41] B.R.B. Scharifker, G. Hills, Theoretical and experimental studies of multiple nucleation, Electrochim. Acta 28 (1983) 879–889.
[42] B.R.B. Scharifker, J. Mostany, Three-dimensional nucleation with diffusion controlled growth. Part I. Number density of active sites and nucleation rates per site, J. Electroanal, Chem. Interfacial Electrochem 177 (1984) 13–23.
[43] Z. Luo, S. Yuchang, S. Yue, Q. Yu, H. Zhang, J. Zhang, Electrodeposition of copper nanopowder with controllable morphology: influence of pH on the nucleation/growth mechanism, J. Solid State Electrochem. 25 (2021) 1–11.
[44] M.T. Pise, M. Muduli, A. Chatterjee, B.P. Kashyap, R.N. Singh, S.S.V. Tatiparti, Instantaneous-progressive nucleation and growth of palladium during electrodeposition, Res. Surf. Interfaces 6 (2022), 100044 (2022).
[45] M. Palomar-Pardavé, B.R. Scharifker, E.M. Arce, M. Romero-Romo, Nucleation and diffusion-controlled growth of electroactive centers. Reduction of protons during cobalt electrodeposition, Electrochim. Acta 50 (2005) 4736–4745.
[46] S. Gu, X. Wang, Y. Wei, B. Fang, Mechanism for nucleation and growth of electrochemical deposition of palladium(II) on a platinum electrode in hydrochloric acid solution, Sci. China Chem. 57 (2014) 755–762.
[47] B.E. Conway, The solvation factor in specificity of ion adsorption at electrodes, Electrochim. Acta 40 (1995) 1501–1512.
[48] Y. Zhang, S. Furyk, L.B. Sagle, Y. Cho, D.E. Bergbreiter, P.S. Cremer, Effects of Hofmeister anions on the LCST of PNIPAM as a function of molecular weight, J. Phys. Chem. C. 111 (2007) 8916–8924.
[49] K.P. Gregory, G.R. Elliott, H. Robertson, A. Kumar, E.J. Wanless, G.B. Webber, V.S. J. Craig, G.G. Andersson, A.J. Page, Understanding specific ion effects and the Hofmeister series, Phys. Chem. Chem. Phys. 24 (2022) 12661–13418.
[50] P. Lo Nostro, V. Mazzini, B.W. Ninham, M. Ambrosi, L. Dei, Specific anion effects on the kinetics of iodination of acetone, ChemPhysChem 17 (2016) 2567–2571.
[51] T.C. Franklin, Some mechanisms of action of additives in electrodeposition processes, Surf. Coat. Technol. 30 (1987) 415–428.
[52] V.S.J. Craig, B.W. Ninham, R.M. Pashley, The effect of electrolytes on bubble coalescence in water, J. Phys. Chem. 97 (1993) 10192–10197.
[53] T.C. Franklin, J.R. Goodwyn, The effect of organic compounds on the codeposition of hydrogen with Nickel, J. Electrochem. Soc. 109 (1962) 288.
[54] N.D. Nikolić, G. Branković, M.G. Pavlović, K.I. Popov, The effect of hydrogen co-deposition on the morphology of copper electrodeposits. II. Correlation between the properties of electrolytic solutions and the quantity of evolved hydrogen, J. Electroanal. Chem. 621 (2008) 13–21.